Published in final edited form as:
Mol Cell Neurosci. 2011 January ; 46(1): 122–135. doi:10.1016/j.mcn.2010.08.012.

The effect of HSP-causing mutations in *SPG3A* and *NIPA1* on the assembly, trafficking, and interaction between atlastin-1 and NIPA1

Emmanuel J. Botzolakis[1,§], **Jiali Zhao**[2,§], **Katharine N. Gurba**[1], **Robert L. Macdonald**[2,3], and **Peter Hedera**[2,3,4,*]

[1]Medical Scientist Training Program, Vanderbilt University, Nashville, TN

[2]Department of Neurology, Vanderbilt University, Nashville, TN

[3]Center for Molecular Neuroscience, Vanderbilt University, Nashville, TN

[4]Center for Human Genetics Research, Vanderbilt University, Nashville, TN

Abstract

Despite its genetic heterogeneity, hereditary spastic paraplegia (HSP) is characterized by similar clinical phenotypes, suggesting that a common biochemical pathway underlies its pathogenesis. In support of this hypothesis, we used a combination of immunoprecipitation, confocal microscopy, and flow cytometry to demonstrate that two HSP-associated proteins, atlastin-1 and NIPA1, are direct binding partners, and interestingly, that the endogenous expression and trafficking of these proteins is highly dependant upon their coexpression. In addition, we demonstrated that the cellular distribution of atlastin-1:NIPA1 complexes was dramatically altered by HSP-causing mutations, as missense mutations in atlastin-1 (R239C and R495W) and NIPA1 (T45R and G106R) caused protein sequestration in the Golgi complex (GC) and endoplasmic reticulum (ER), respectively. Moreover, we demonstrated that HSP-causing mutations in both atlastin-1 and NIPA1 reduced axonal and dendritic sprouting in cultured rat cortical neurons. Together, these findings support the hypothesis that NIPA1 and atlastin-1 are members of a common biochemical pathway that supports axonal maintenance, which may explain in part the characteristic degeneration of long spinal pathways observed in patients with HSP.

INTRODUCTION

Hereditary spastic paraplegia (HSP) is a group of neurodegenerative disorders characterized by progressive spastic weakness of the lower extremities ([Fink 2006], [Züchner 2007] and [Salinas et., 2008]). Retrograde degeneration of spinal ascending (dorsal columns) and descending (corticospinal tracts) pathways is the pathologic hallmark of this syndrome, suggesting that long axons in the central nervous system are most vulnerable ([Wharton et al., 2003] and Deluca et al., 2004]). Consistent with this hypothesis, disruption of axonal

*Author for correspondence: Department of Neurology, Vanderbilt University, 465 21st Avenue South, 6140 MRB III, Nashville, TN, 37232- 8552 Phone: 615-936-3920; Fax: 615-322-5517; peter.hedera@vanderbilt.edu.
§These authors contributed equally to the work.

transport has been implicated in the pathogenesis of HSP ([Reid 2003] and [Soderblom and Blackstone, 2006]). Interestingly, while the pathological features of HSP are relatively uniform, mutations in more than 40 genes have been identified thus far, making it one of the most genetically heterogeneous neurodegenerative disorders ([Fink 2006] and [Züchner 2007]). This implies the existence of a common biochemical pathway central to the pathogenesis of HSP. However, it remains unclear which HSP-associated gene products interact directly, and how mutations alter these interactions to produce the clinical phenotype.

Atlastin-1, an integral membrane protein encoded by the gene *SPG3A*, belongs to the dynamin superfamily of large GTP-ases. Missense mutations in atlastin-1 are the second most common cause of autosomal dominant (AD) HSP ([Zhao et al., 2001], [Tessa et al., 2002], [Abel et al., 2004], [Durr et al., 2004], [Hedera et al., 2004], and [Sauter et al., 2004]), and most of these mutations are clustered in or around the GTP-ase domain, resulting in loss of catalytic activity ([Zhao et al., 2001], [Durr et al., 2004] and [Abel et al., 2004]). How this loss of function causes AD HSP, however, is only beginning to be understood. Atlastin-1 is important for the formation of the tubular endoplasmic reticulum (ER) network, and HSP mutations inhibit tubule interconnections ([Hu et al., 2009] and [Orso et al., 2009]). However, whether this is the main pathogenic mechanism remains unknown; atlastin-1 can be also found in other subcellular compartments, including cell surface, dendrites and axons ([Zhu et al., 2003], [Namekawa et al., 2007] and [Rismanchi et al., 2008]). Based on its known homology to the dynamin superfamily, atlastin-1 has been suggested to participate in protein trafficking (Praefcke and McMahon, 2004). Additionally, atlastin-1 is enriched in neuronal growth cones, and knockdown of atlastin-1 expression impaired axonal elongation (Zhu et al., 2006). Recent evidence in *Drosophila* suggested that atlastin-1 may be important for synapse formation (Lee et al., 2009). Interestingly, this role was dependent upon the ability of atlastin-1 to interact directly with the microtubule-severing protein spastin ([Evans and et al., 2006] and [Sanderson et al., 2006]), mutations in which are the most common cause of AD HSP (Hazan et al., 1999).

Missense mutations in NIPA1 (non-imprinted gene in Prader-Willi/Angelman syndrome region 1), an integral membrane protein encoded by the gene *SPG6*, are additional important causes of AD HSP ([Rainier et al., 2003], [Chen et al., 2005], [Reed et al., 2005] and [Kaneko et al., 2006]). NIPA1 is mostly expressed in early endosomes and on the cell surface, where it is thought to serve as a magnesium transporter; however, we previously demonstrated the presence of endogenous NIPA1 protein in the Golgi complex (GC) as well ([Goytain et al., 2007] and [Zhao et al., 2008]). It remains unclear if disruption of magnesium transport due to pathogenic mutations directly contributes to HSP pathogenesis, or if mutations alter other properties of the mutant protein. One possible mechanism of axonal degeneration caused by NIPA1 mutations is inhibition of bone morphogenic protein (BMP)-linked signaling pathways, even though a more robust phenotype was observed in knock down expression of NIPA1 than in NIPA1 HSP mutations ([Wang et al., 2007] and [Tsang et al., 2009]). Our previous work using cultured rat neurons and a *Caenorhabditis elegans* model suggested a toxic gain of function with endoplasmic reticulum stress triggering programmed cell death through the unfolded protein response (Zhao et al., 2008). Whether NIPA1 interacts with other HSP-associated proteins is not yet known.

Here, using a combination of confocal microscopy, immunoprecipitation, knock-down expression using RNA interference, and flow cytometry, we demonstrated that endogenous atlastin-1 and NIPA1 are direct binding partners, an interaction that appears to be required for expression of atlastin-1, but not NIPA1, on the cell surface. Knock-down expression of NIPA1 resulted in marked reduction of atlastin-1 in neuronal processes. Moreover, we demonstrated that HSP-associated missense mutations in atlastin-1 (R239C and R495W)

and NIPA1 (T45R and G106R) dramatically alter the cellular distribution of both proteins, both in heterologous expression systems and in cultured primary cortical neurons. Finally, we demonstrated that HSP-associated mutations alter neuronal growth properties, as measured by a neuronal branching assay. Taken together, these findings support the idea that a common biochemical pathway underlies the pathogenesis of HSP, and warrant systematic evaluation of possible interactions between other HSP-associated proteins. Indeed, further characterization of this pathway should not only improve our understanding of axonal maintenance, but should also provide new therapeutic options for the treatment of HSP.

RESULTS

NIPA1 and atlastin-1 were colocalized and were binding partners

Previous studies have shown that NIPA1 and atlastin-1 have widespread intracellular localization, including the ER and GC ([Zhu et al., 2003], [Zhao et al., 2008] and [Rismanchi et al., 2008]). Consistent with these findings, we found that expression of recombinant NIPA1-GFP and atlastin-1-myc in heterologous cells yielded significant co-localization in the ER and GC, with additional partial co-localization in the cytoplasm (Figure 1, panels A–C). The presence of both proteins in the GC was confirmed by triple immunostaining using the Golgin 245 marker (Figure 2, panels A–D, calnexin staining not shown). The observed colocalization of epitope-tagged proteins was confirmed by antibody staining of endogenous NIPA1 and atlastin-1 proteins in cultured rat cortical neurons. Although compartmentalization was more easily observed in heterologous cells, significant overlap of these two proteins in cultured rat cortical neurons was also observed, including in axons (Figure 3, panels A–D).

Interestingly, while previous studies have demonstrated that NIPA1 reaches the cell surface when expressed alone ([Goytain et al., 2007] and [Zhao et al., 2008]), cell surface expression of atlastin-1 has yet to be reported. However, our confocal microscopy studies clearly identified both NIPA1:GFP and atlastin-1:myc on the cell surface (Figures 1 and 2). This raised concerns that the myc epitope was somehow generating a non-specific signal on the cell surface. To test this hypothesis, we expressed the protein spastin, which is known to have only nuclear and cytosolic localization (Errico et al., 2002), in a myc-tagged form. Consistent with previous data, spastin was not detected on the cell surface (data not shown). Moreover, we were able to detect untagged atlastin-1 on the cell surface using an antibody against the native protein in the same region containing the myc epitope (see flow cytometry results, below).

The significant colocalization of endogenous NIPA1 and atlastin-1 proteins prompted us to investigate whether or not these proteins were *in vivo* binding partners. Immunoprecipitation experiments from whole mouse brain demonstrated that these proteins formed hetero-complexes, as both proteins could be pulled down when the other putative binding partner was used as bait (Figure 3, panels E and F). Of note, neither protein could be pulled down using antibodies to an unrelated membrane protein, the $GABA_A$ receptor β3 subunit (data not shown), suggesting that the interaction between NIPA1 and atlastin-1 proteins was specific.

HSP-associated mutations in NIPA1 and atlastin-1 altered the subcellular distribution of both proteins without altering their assembly

We previously demonstrated that the HSP-causing T45R and G106R mutations in NIPA1 (located in the first and third transmembrane domains, respectively) caused accumulation of mutant protein in the ER and led to apoptotic cell death by triggering the unfolded protein response (Zhao et al., 2008). Consistent with these findings, we observed significant ER

retention (assessed by co-localization with calnexin) of NIPA1-GFP T45R and G106R mutants when co-expressed with WT atlastin-1-myc (Figure 2, panels M–T). Furthermore, both NIPA1-GFP mutants substantially altered the subcellular distribution of co-expressed WT atlastin-1-myc, causing it to accumulate in the ER as well (Figure 2, panels M–T). Of note, overexpression of WT atlastin-1-myc in neuronal and heterologous cell lines did not modify the cellular phenotype induced by mutant forms of NIPA1-GFP protein, and the dynamics of the apoptotic response were similar to those observed when mutant NIPA1-GFP was expressed alone (data not shown).

Given the considerable allelic heterogeneity of atlastin-1 mutations, we chose previously-studied mutations in the highly conserved GTP-ase domain (R239C) and the first transmembrane domain (R495W) for further analysis (Namekawa et al., 2007). As observed with mutations in NIPA1-GFP, mutations in atlastin-1-myc significantly altered the subcellular distribution of both atlastin-1-myc and WT NIPA1-GFP (Figure 1, panels J–O; Figure 2, panels E–L). Indeed, compared to the fine reticular and punctate expression pattern seen with WT atlastin-1-myc, the expression pattern of atlastin-1-myc mutants was characterized by thick intracellular bundles and aggregates. In addition, mutant forms of atlastin-1 caused WT NIPA1 to accumulate in the GC, reducing its degree of cytoplasmic expression (Figure 1, panels J–O, Figure 2, panels E–L).

We next analyzed the effect of HSP-causing mutations in NIPA1 and atlastin-1 on the ability of these proteins to assemble. Interestingly, neither the R239C nor the R495W mutation in atlastin-1 altered the ability of NIPA1-HA to immunoprecipitate atlastin-1-myc (Figure 3). The same was also true with the T45R and G106R mutations in NIPA1 (data not shown). Thus, HSP-causing mutations led to resdistribution of atlastin-1:NIPA1 complexes, but did not affect their assembly.

Co-transfection of NIPA1 and atlastin-1 increased the levels of atlastin-1, but not NIPA1, surface expression

Quantifying protein expression with microscopy is inherently challenging (particularly surface expression), as the process is extremely low throughput and highly operator dependent. We therefore turned to flow cytometry, which allows for rapid, unbiased quantitation of surface and total cellular expression in large populations of cells ([Zhao et al., 2008] and [Lo et al., 2008]). Using this approach, we aimed to better understand how co-expression of NIPA1 and atlastin-1 affected surface or total protein levels, and importantly, how these levels were affected by HSP-causing mutations.

When transfected alone, WT atlastin-1-myc was expressed poorly on the cell surface (Figure 4A), and this level of expression was not affected significantly by either of the atlastin-1 HSP-associated mutations (data not shown). This was not secondary to poor cellular expression of our atlastin-1-myc construct, as permeabilizing cells prior to staining revealed significant amounts of protein (Figure 4A). Co-transfection with NIPA1-HA, however, increased surface expression of WT atlastin-1-myc approximately 10-fold (Figure 4A). Interestingly, this did not affect total cellular expression levels, indicating that co-expression of atlastin-1-myc with NIPA1-HA markedly decreased the intracellular pool of atlastin-1-myc (Figure 4A). With these assays, however, we could not determine whether this was secondary to an increased rate of trafficking to the cell surface or a decreased rate of internalization from the cell surface. NIPA1-HA, on the other hand, was efficiently expressed on the cell surface when transfected alone and was not substantially affected either by co-transfection with atlastin-1-myc (Figure 4B) or, based on our previous work using this same experimental approach, by the introduction of HSP-associated mutations (Zhao et al., 2008). The same was true for NIPA1-HA total cellular expression (Figure 4B).

Of note, detection of myc-tagged atlastin-1 protein on the cell surface (i.e., positive staining in the absence of membrane permeabilization) implied that the C-terminus was located extracellularly, in contrast to the predicted intracellular orientation (Hu et al., 2009). To exclude the possibility that the myc epitope was altering the membrane orientation of the atlastin-1 protein, we probed for surface expression using an antibody against the native C-terminus of atlastin-1 (amino acids 514–550). While the results differed somewhat quantitatively from those obtained with the myc epitope, the presence of a positive signal nevertheless confirmed the extracellular orientation of the C-terminus (Figure 4C).

An HSP-associated mutation in the GTP-ase domain of atlastin-1 exerted a potent dominant negative effect on WT NIPA1 cell surface expression

Using our flow cytometry assay, we next evaluated the effects of HSP-associated mutations on surface and total cellular levels of NIPA1-HA and atlastin-1-myc in the setting of co-expression (Figure 5). While the NIPA1 T45R mutation was previously shown to decrease surface levels of NIPA1-HA when expressed alone ([Zhao et al., 2008]), it had no effect on surface or total cellular levels of NIPA1-HA when co-expressed with atlastin-1-myc. The same was true for the NIPA1 G106R mutation and for the atlastin-1 R495W mutation. In contrast, the atlastin-1 R239C mutation significantly decreased surface levels of both atlastin-1-myc and co-expressed NIPA1-HA. This reduction in surface expression occurred in the setting of minimally decreased total expression levels of NIPA1-HA and atlastin-1-myc, indicating that the intracellular pools of both proteins had increased. Interestingly, the observed reduction in surface expression was nearly the same for both NIPA1-HA and atlastin-1-myc (~60%), suggesting that the R239C mutation promoted intracellular retention of atlastin-1:NIPA1 protein complexes.

Knocking down expression of endogenous NIPA1 in rat cortical neurons altered the cellular distribution of endogenous atlastin-1 protein

The observed dependence of atlastin-1 surface trafficking on coexpression with NIPA1 in heterologous cells prompted us to further explore this relationship in primary neuronal cultures. We therefore generated several siRNA constructs targeted against the endogenous NIPA1 transcript (see Methods), identified the two most efficacious in knocking down expression (siRNA2 and siRNA4; Supplementary Figure 1), and used confocal microscopy to monitor atlastin-1 subcellular localization. Consistent with our results in heterologous cells, rat cortical neurons expressing the two most efficacious NIPA1 siRNAs showed abnormal subcellular distribution of endogenous atlastin-1, with clumping of endogenous atlastin-1 in the cell soma. In addition, atlastin-1 was absent from the cell surface and, most notably, in the neuronal processes (Figure 6, panels A–C). We also addressed the question of whether this alteration of atlastin-1 cellular trafficking was due to a non-specific disruption of the secretory pathway. Morphology of ER and GC did not differ in neurons expressing siRNAs targeting NIPA1 protein from control neurons (data not shown). Rather than rely on morphologic analysis alone, we also analyzed cell surface trafficking of the $GABA_A$ receptor α1 subunit as a marker of secretory pathway function [Ding et al., 2010]. We found that neurons expressing NIPA1 siRNAs had similar levels of $GABA_A$ receptor α1 subunit on the cell surface compared to transfection of empty vector, suggesting that the effect of NIPA1 knock-down on cellular trafficking of atlastin-1 was not an experimental artifact (Figure 6, panels G–I).

HSP-causing mutations in atlastin-1 altered distribution, but not expression, of WT NIPA1 in cultured rat cortical neurons

In heterologous cells, HSP-causing mutations in atlastin-1 had profound effects on the cellular distribution of both proteins. To determine if the same was true in primary neuronal cultures, we overexpressed mutant atlastin-1 protein in rat cortical neurons and monitored

the expression of atlastin-1 and NIPA1 using confocal microscopy. Consistent with our aforementioned experiments in heterologous cells (Figure 1, panels A–C), there was significant co-localization of WT NIPA1 and WT atlastin-1 in both neuronal bodies and processes (Figure 7 and 8, panel A). However, in the setting of HSP-causing atlastin-1 mutants, the degree of co-localization between NIPA1 and atlastin-1 was markedly reduced. In addition, NIPA1 expression was nearly eliminated from neuronal processes, especially in axons (Figure 7 and 8, panel B and C).

To determine whether the altered pattern of NIPA1 expression was associated with alterations in total cellular expression levels, Western blot analysis was performed on whole-cell lysates obtained from cultured rat cortical neurons expressing either WT or mutant forms of atlastin-1-myc (Figure 9A–C). When normalized to endogenous actin levels, the total amount of endogenous NIPA1 (Figure 9, panel B) did not differ in the presence of WT atlastin-1 (Figure 9, panel A, lane 1), HSP-causing atlastin-1 mutations (Figure 9, lane 2 and 3), or empty vector (Figure 9, lane 4). Of note, the results for overexpressed WT NIPA1-HA were nearly identical (data not shown). Thus, HSP-causing mutations in atlastin-1 altered the normal trafficking of NIPA1 without altering the absolute levels of protein expression, as was observed in heterologous cells (Figure 1, panels J–O).

HSP-causing mutations in atlastin-1 reduced neuronal branching

In agreement with previous reports ([Zhu et al., 2006]), we noted high levels of WT atlastin-1 expression in axonal growth cones. In the setting of HSP-causing mutations, however, expression of atlastin-1 in growth cones was considerably reduced (Figure 7 and 8). As with NIPA1, this was most likely due to alterations in protein trafficking, as the total amounts of WT and mutant atlastin-1 did not differ based on Western blot analysis (Figure 9, panel C). Of note, the presence of mutant forms of atlastin-1 did not alter the survival of cultured rat cortical neurons followed up to 14 days following transfection, as determined by LDH assays (Zhao et al., 2008) (data not shown).

To determine how the altered expression of atlastin-1 and NIPA1 in neuronal processes affected neuronal growth properties, we performed a semiquantitative analysis of neuronal branching. Interestingly, in the presence of mutant forms of atlastin-1, the degree of neuronal branching was markedly reduced when assayed 14 days after transfection (Figure 9, panel D; WT: 9.42 ± 2.18, R239C: 4.94 ± 1.29, R495W: 5.39 ± 2.03; $p<0.01$; the difference between the two mutations was not statistically significant). This was not obvious 48 hours after transfection when neurons expressing these constructs had similar amounts of branching (WT: 3.33 ± 1.31, R239C: 2.86 ± 1.25, R495W: 2.89 ± 1.39, differences not statistically significant). Overexpression of WT NIPA1-HA did not rescue the phenotype, as the degree of branching reduction was similar for neurons co-transfected with WT NIPA1-HA (Figure 9, panel D; WT: 8.89 ± 2.22, R239C: 5.06 ± 1.27, R495W: 5.11 ± 2.25; $p<0.01$).

HSP-causing mutations in NIPA1 reduced neuronal branching

We previously described significant cell death consistent with apoptosis in heterologous and homologous cell lines expressing T45R or G106R mutations (Zhao et al., 2008). The proportion of cultured rat cortical neurons underwent apoptosis within three days after transfection with T45R or G106R GFP-tagged NIPA1 constructs, though a fraction (~10–15%) survived for a longer period of time without any observable morphologic changes at the level of the cell soma. These neurons, however, displayed a significant reduction in branching compared to neurons transfected with GFP-tagged WT NIPA1 (WT: 8.21 ± 1.78, T45R: 3.88 ± 1.68, G106R: 4.11 ± 1.93; $p<0.01$ monitored at 14 days in culture; the difference between the two mutations was not statistically significant) (Figure 8 G–J). This

effect of NIPA1 mutations within the surviving neurons appeared progressive, as few differences were present 48 hours post-transfection comparing to WT NIPA1 (branching – WT: 3.21 ± 1.12, T45R: 2.88 ± 1.15, G106R: 3.02 ± 1.52, differences not statistically significant; NIPA1-GFP positive structures – WT: 7.83 ± 2.23, T45R: 8.43 ± 3.01, G106R: 7.89 ± 3.44, differences not statistically significant) (Figure 9G). Branching of neurons transfected with WT NIPA1 and empty vector showed essentially the same degree of dendritic sprouting 2 and 14 days post-transfection, suggesting that the impact of mutations was on maintenance of neuronal branching, as opposed to its initiation. We also observed that the number of GFP positive NIPA1-associated puncta within individual neuronal processes was reduced at 14 days in culture (WT: 43.27 ± 11.83, T45R: 10.81 ± 6.43, G106R: 13.94 ± 8.83; $p<0.01$; the difference between the two mutations was not statistically significant) (Figure 9H). Overexpression of WT atlastin-1 did not modify this cellular phenotype (data not shown).

DISCUSSION

The goals of this study were to explore the possibility that two proteins implicated in the pathogenesis of HSP, atlastin-1 and NIPA1, were part of a common biochemical pathway, and to determine if disease-causing mutations in these proteins affected their assembly, expression, and trafficking. Consistent with this hypothesis, our results provide evidence that atlastin-1 and NIPA1 are binding partners, and moreover, that this interaction is required for efficient trafficking of atlastin-1 to the cell surface. The converse did not appear to be true, as high levels of NIPA1 were identified on the cell surface independent of the presence of atlastin-1. Of note, a direct interaction between HSP-causing proteins has only previously been demonstrated for atlastin-1, receptor expression enhancing protein 1 (REEP1), and spastin, a microtubule severing protein ([Evans et al., 2006], [Sanderson et al., 2006] and [Park et al., 2010]). Our results thus raise several important questions including 1) are all four of these proteins are co-assembled *in vivo*, 2) if so, to what degree and in which cellular compartments; 3) are other HSP-associated proteins such as spartin or maspardin ([Patel et al., 2002] [Simpson et al., 2003]) also part of this pathway, and 4) exactly how does disruption of this pathway affect axonal maintenance, which has been suggested in multiple studies to be the hallmark of HSP ([Züchner 2007] and [Salinas et al., 2008]).

Interestingly, HSP-causing mutations in NIPA1 (T45R and G106R) and atlastin-1 (R293C and R495W) did not significantly affect the ability of these proteins to interact. Indeed, while the mutations had profound effects on the cellular distributions of both NIPA1 and atlastin-1 (significant sequestration in the ER and GC, respectively), none of the mutations significantly altered the amount of atlastin-1 immunoprecipitated with NIPA1. Consistent with this observation, the atlastin-1 R239C mutation reduced surface expression of both NIPA1 and atlastin-1 by nearly the same extent, suggesting that forward trafficking of the assembled NIPA1:atlastin-1 protein complex was impaired. Together, these results indicate that assembly of NIPA1 and atlastin-1 occurs very early in the secretory pathway (possibly as early as the ER), and moreover, that the primary consequence of these HSP-causing mutations is not to alter the ability of these proteins to interact, but rather, to alter the cellular distribution of the atlastin-1:NIPA1 complex. That being said, it should be noted that by confocal microscopy, all of the HSP-causing mutations decreased the extensive colocalization of atlastin-1 and NIPA1 observed in the WT condition. Decreased colocalization in the setting of similar co-immunoprecipitation suggests that only a fraction of the total amount of atlastin-1 and NIPA1 proteins were actually assembled in the WT condition, the remainder being unassembled and differentially sensitive to the HSP-causing mutations.

One of the more unexpected results of this study was the observation that HSP-causing mutations in atlastin-1 gave rise to nearly identical molecular and cellular phenotypes, despite being located in entirely different protein domains (the R239C mutation is located in the GTP-ase domain and the R495W mutation is located in the second transmembrane domain). Indeed, both mutations caused a redistribution of NIPA1 and atlastin-1 with notable sequestration in the GC, and both mutations reduced neuronal branching in cultured rat cortical neurons. There was, however, one notable difference between these mutations identified by our flow cytometric assay of surface expression in heterologous cells. While the R239C mutation had a dominant negative effect on the surface expression of co-expressed WT NIPA1, this was not observed for the R495W mutation, suggesting that the GTP-ase domain may be particularly important for forward trafficking of assembled NIPA1:atlastin-1 protein complexes. That being said, both atlastin-1 mutations had potent dominant negative effects on NIPA1 expression in synaptic boutons, a difference that may reflect either the unique molecular environment found in neuronal processes or the artificial nature of heterologous expression systems. We favor the former hypothesis, as the remainder of the cellular effects were nearly identical in HEK293T cells and cultured rat cortical neurons.

Much like HSP-causing mutations in atlastin-1, HSP-causing mutations studied in NIPA1 had profound effects on the cellular distribution of both proteins without significantly affecting total cellular expression levels. However, the patterns of protein expression were markedly different. While mutations in atlastin-1 caused protein sequestration in the GC, those in NIPA1 caused protein sequestration in the ER, a finding shown in previous studies to cause programmed cell death via a toxic gain-of-function mechanism (Zhao et al., 2008). This may explain why HSP caused by mutations in NIPA1 (SPG6) presents with greater severity than HSP caused by mutations in atlastin-1 (SPG3A), despite the clinical findings being similar overall. Indeed, while SPG3A typically presents in childhood with relatively slow progression, SPG6 presents in adulthood with an aggressive course, leading to wheelchair dependency in most patients ([Fink and Hedera, 1999], [Zhao et al., 2001], [Tessa et al., 2002], [Rainier et al., 2003], [Durr et al., 2004], [Hedera et al., 2004], [Sauter et al., 2004], [Abel et al., 2004], [Chen et al., 2005], [Reed et al., 2005] and [Kaneko et al., 2006]). These clinical differences are supported by MRI volumetric studies, which found minimal spinal cord atrophy in SPG3A patients but profound spinal cord atrophy in SPG6 patients (Hedera et al., 2005). However, further studies will be necessary to determine if differences in the cellular distribution of mutant HSP proteins are actually responsible for these phenotypic differences. In other words, are phenotypic differences the result of different amounts of atlastin-1 and/or NIPA1 being delivered to a subset of subcellular compartments, or do they reflect intrinsically different properties of mutant atlastin-1 and NIPA1 proteins? Indeed, these proteins may differentially interact with other neuronal proteins, which may modify the disease phenotype. For example, recent studies have demonstrated that NIPA1 plays an important inhibitory role in BMP signaling by binding to BMP receptors and promoting endocytosis and lysosomal degradation, an effect impaired by HSP-causing mutations in NIPA1 ([Wang et al., 2007] and [Tsang et al., 2009]). Interestingly, the HSP-associated proteins spastin and spartin were also shown to interact directly with BMP receptors; however, whether or not atlastin-1 also has this capacity is currently unknown.

Atlastin-1 plays an important role in the development of both the ER and GC ([Hu et al., 2009] and Orso et al., 2009]), where it interacts with REEP1 and spastin and coordinates ER morphogenesis and microtubule dynamics (Park et al., 2010). These abnormalities in tubular ER shaping and network interactions have been suggested to be the main mechanism of axonal degeneration in HSP. However, we do not know if the NIPA1 interaction with atlastin-1 is involved in the same process. Furthermore, the function of atlastin-1 in other

subcellular compartments, including in the cell surface membrane, remains also unknown. The NIPA1 and atlastin-1 interaction was especially important for the trafficking of atlastin-1 to the cell surface, and depletion of endogenous NIPA1 dramatically altered the intraneuronal distribution of atlastin-1. Atlastin-1 is enriched in intracellular membranes and its C-terminus is localized in the cytoplasm. The detection of atlastin-1 by antibodies against the C-terminus on the cell surface indicates that C-terminus may be also extracellular, and its normal function on the cell surface and the role in HSP pathogenesis will be addressed in future studies.

In summary, we have shown that 1) atlastin-1 and NIPA1 HSP proteins are binding partners, 2) NIPA1 facilitates cell surface trafficking of atlastin-1, 3) HSP-causing mutations in atlastin-1 and NIPA1 alter the trafficking but not the assembly of these proteins, 4) HSP-causing mutations in atlastin-1 exhibit dominant negative effects on WT NIPA1, and 5) mutant forms of atlastin-1 and NIPA1 result in reduced outgrowth of cultured cortical rat neurons. Our results suggest that atlastin-1 and NIPA1 are members of the same biochemical pathway, and that alterations in the cellular distribution of atlastin-1:NIPA1 complexes may be involved in the pathogenesis of HSP.

METHODS

Eukaryotic DNA expression constructs

The generation of the full coding sequence construct of the *NIPA1* was described previously ([Zhao et al. 2008]). The full length of *atlastin-1* construct was a gift from Dr.Blackstone ([Zhu et al., 2003]). T45R and G106R missense mutations in NIPA1 construct, and R239C and R495W missense mutations in the atlastin-1 construct were introduced using a site-directed mutagenesis kit (QuickChange, Stratagene, La Jolla, CA) and verified by sequencing.

Cell Culture and expression of recombinant Atlastin-1 and NIPA1

HEK293T cells and COS7 cells (American Type Culture Collection, Manassas, VA) were maintained at 37°C in humidified 5% CO_2 / 95% air using Dulbecco's Modified Eagle Medium (Invitrogen) supplemented with 10% fetal bovine serum (Invitrogen), 100 IU/ml penicillin (Invitrogen), and 100 μg/ml streptomycin (Invitrogen). Cells were plated at a density of ~10^6 cells per 6 cm culture dish (Corning Glassworks) and transfected ~24 hours later with 1 μg of cDNA per construct using FuGene6 (Roche Diagnostics) according to manufacturer recommended protocol. Blank pcDNA3.1+ vector was added to maintain a constant amount of cDNA in each transfection condition.

Primary cortical neuronal cultures were prepared from embryonic day 18 (E18) rat embryos and transfected using the rat neuron nucleofector kit (Amaxa Inc, Gaithersburg, MD) according to the manufacturer's protocol. The primary cortical neurons were electrically transfected with the respective constructs using the nucleofactor 1 device and the manufacturer's optimized protocol.

Flow cytometry

Cells were harvested 24 h after transfection using 37°C trypsin/EDTA (Invitrogen) and placed immediately in 4°C FACS buffer composed of PBS (Mediatech), 2% fetal bovine serum (FBS) (Invitrogen), and 0.05% sodium azide (VWR). Cells were then transferred to 96-well plates, where they were washed twice in FACS buffer (i.e., pelleted by centrifugation at 450 × g, vortexed, and resuspended). For surface protein staining, cells were incubated in antibody-containing FACS buffer for 1 h at 4°C, washed in FACS buffer three times, and resuspended in 2% w/v paraformaldehyde (PFA) (Electron Microscopy

Sciences). For total protein staining, samples were first fixed and permeabilized using Cytofix/Cytoperm (BD Biosciences) for 15 min. After washing twice with Permwash (BD Biosciences) to remove residual fixative, cells were resuspended in antibody-containing Permwash for 1 h at 4°C. Following incubation with antibody, samples were washed four times with Permwash and twice with FACS buffer before resuspension in 2% PFA. The HA antibody (clone 16B12) was obtained from Covance as an Alexa-647 conjugate and used at a 1:250 dilution for surface staining and a 1:500 dilution for total protein staining. The MYC antibody (clone 4A6) was obtained from Millipore as an Alexa-555 conjugate and used at a 1:250 dilution for surface staining.

Samples were run on a LSR II flow cytometer (BD Biosciences). For each staining condition, 50,000 cells were analyzed. Nonviable cells were excluded from analysis based on forward- and side-scatter profiles (data not shown), as determined from staining with 7-amino-actinomycin D (7-AAD) (Invitrogen). The Alexa-555 fluorophore was excited using a 535 nm laser and detected with a 575/26 bandpass filter. The Alexa-647 fluorophore was excited using a 635 nm laser and detected with a 675/20 bandpass filter. Data were acquired using FACSDiva (BD Biosciences) and analyzed off-line using FlowJo 7.1 (Treestar). To compare surface and total expression levels of wild-type (WT) and mutant proteins, the mean fluorescence intensity of mock transfected cells was subtracted from the mean fluorescence intensity of each positively transfected condition. The remaining fluorescence was then normalized to that of the WT condition, yielding a relative fluorescence intensity ("Relative FI"). Statistical significance was determined using a one-sample t-test using a hypothetical mean of 1 (since data in each condition were normalized to WT expression). Data were expressed as mean ± SEM.

Immunocytochemistry and confocal microscopy

Antibodies used in this study included mouse monoclonal anti-HA antibodies (Sigma-Aldrich, St. Louis, MO), calnexin antibodies, Golgi 58K antibodies, (all from Abcam, Cambridge, MA) and mouse monoclonal Cy3 antibodies (Rockland, Gilbertsville, PA). Generation and characterization of polyclonal anti-NIPA1 antibodies was described previously ([Zhao et al., 2008]). Atlastin-1 rabbit antibodies against amino acids 514–550 were purchased from Santa Cruz Biotechnology (Santa Cruz, CA). Cells were fixed with 4% paraformaldehyde (Electron Microscopy Sciences, Fort Washington, PA) and blocked with 2% bovine serum albumin in 1× PBS containing 0.5% Triton X-100. Cells were incubated with the specific antibody at a dilution of 1:800. After two hours of incubation, cells were washed twice with 1× PBS and incubated with the secondary antibody conjugated to Cy3 for 1 hour. After three washes, coverslips were mounted onto microscope slides and fluorescent images acquired with a Zeiss LSM510 META laser-scanning confocal microscope and processed with LSM Image software. Transfected cells were evaluated in a blind fashion in regards of the presence of WT, mutant forms or sham transfections; we evaluated between 50 and 100 cells for each construct and specific numbers can be found in the Results section. Images were visualized using a confocal microscope and the LSM images were photographed at 20×, 40×, 60×, and 100× magnification. LSM images were photographed at 20×, 40×, 60×, and 100× magnification.

Neuronal branching of transfected rat cortical neurons was analyzed 48 hours and 14 days after transfection. Primary and secondary neuronal dendritic branches in neurons stained with microtubule-associated protein 2 antibodies (MAP2-A4, Santa Cruz Biotechnology) were counted in a blind fashion to the transfected construct, and 100 cells for each construct were analyzed. We compared the total sum of both primary and secondary branching. GFP-positive vesicular structures in the neuronal processes were analyzed in a similar manner. The number of observed branches and number of GFP-positive structures were compared using an unpaired Student's *t*-test.

Immunoprecipitation and Western blot analysis

For immunoprecipitation of endogenous proteins, mouse brain tissue lysates were prepared from adult c57 male mouse brain. The brain tissue was homogenized in M-PER protein extraction reagent (PIERCE) with the protease inhibitor cocktail (Roche). The lysate was then centrifuged at 15000prm/4c/10min. The supernatant was either incubated with 6ug of anti-NIPA1 antibodies or the same concentration of control Goat IgG, and 30ul protein A agarose beads, or with 6 ug of anti-Atlastin-1 antibodies, or the same concentration of control rabbit IgG, and 30ul protein A agarose beads at 4 C degrees over-night. The beads were washed by wash buffer and the proteins were resolved by SDS-PAGE and immunoblotted with the following antibodies: goat polyclonal anti- NIPA1 (A-12, Santa Cruz) and rabbit polyclonal anti-Atlastin-1 (H-37, Santa Cruz).

For immunoprecipitation of expressed tagged proteins, HEK-293 cells were transfected with a mixture of NIPA1WT-myc and atlastin-1WT-HA or NIPA1-myc mutations NIPA1T45R or G106R and atlastin-1WT-HA, or atlastin-1-myc R239C and R495W mutations with NIPA1WT-myc, or an empty vector as a control. After 36h of transfection, cells were lysated and immuno-precipitated with anti-HA agarose (Thermo scientific, Rockford IL 61101). Cell lysates were used as protein input control of IP, together with actin immunoblotting as a loading control. Quantification of Western blots for the determination of expressed levels of endogenous NIPA1 protein was performed with ChemiImager 5500 (Alpha Innotech) using Alpha Ease Fc software (Alpha Innotech).

NIPA1 protein depletion by siRNA knock-down expression

siRNA oligonucleotides targeting rat NIPA1 (directed against sequence NM_001107519.1) were ordered from Santa Cruz Biotechnology and the following siRNAs were cloned into pGFP-V-RS plasmid with eGFP reporter and then tested:

siRNA1 - CCAAGTCCGAGAGCGTGACCAGTCAGGCT,

siRNA2 - TGCAGCATCATTGTCCAATTCAGGTACAT,

siRNA3 - AGGAGAAGCTGACCAATCCAGTGTTTGTG, and

siRNA4 - CTGGAGTGCTTCGACTCCTCTGTGTTTGG,

As a negative control we used plasmid-A (sc-108060), encoding a scrambled shRNA sequence that will not lead to the specific degradation of any cellular message, also obtained from Santa Cruz Biotechnology. The efficacy of NIPA1 protein depletion was tested transfected cultured primary cortical neurons. 48 hours after transfection we performed cell sorting by flow cytometry and 2×10^6 GFP-positive cells were selected for each tested siRNA and control experiments. The cells were lysed and Western blot with NIPA1 antibodies was performed as described above. We selected two different siRNA, which showed the most effective endogenous NIPA1 protein depletion.

Supplementary Material

Refer to Web version on PubMed Central for supplementary material.

Acknowledgments

This work was supported by K02NS057666 (NIH/NINDS) and by the Spastic Paraplegia Foundation to PH. We gratefully acknowledge the use of the Vanderbilt University Medical Center Cell Imaging Core Resource. The Vanderbilt University Medical Center Cell Imaging Core Resource is supported by National Institutes of Health Grants CA68485 and DK20593.

REFERENCES

Abel A, Fonknechten N, Hofer A, Dürr A, Cruaud C, Voit T, Weissenbach J, Brice A, Klimpe S, Auburger G, et al. Early onset autosomal dominant spastic paraplegia caused by novel mutations in SPG3A. Neurogenetics 2004;5:239–423. [PubMed: 15517445]

Chen S, Song C, Guo H, Xu P, Huang W, Zhou Y, Sun J, Li C,X, Du Y, Li X, et al. Distinct novel mutations affecting the same base in the NIPA1 gene cause autosomal dominant hereditary spastic paraplegia in two Chinese families. Hum. Mutat 2005;25:135–141. [PubMed: 15643603]

Deluca G,C, Ebers G,C, Esiri M,M. The extent of axonal loss in the long tracts in hereditary spastic paraplegia. Neuropathol. Appl. Neurobiol 2004;30:576–84. [PubMed: 15540998]

Ding L, Feng H,J, Macdonald R,L, Botzolakis E,J, Hu N, Gallagher M,J. $GABR_A$ receptor α1 subunit mutation A322D associated with autosomal dominant juvenile myoclonic epilepsy reduces the expression and alters the composition of wild type $GABR_A$ receptors. J. Biol. Chem 2010;285:26390–26405. [PubMed: 20551311]

Durr A, Camuzat A, Colin E, Tallaksen C, Hannequin D, Coutinho P, Fontaine B, Rossi A, Gil R, Rousselle C, et al. Atlastin1 mutations are frequent in young-onset autosomal dominant spastic paraplegia. Arch. Neurol 2004;61:1867–72. [PubMed: 15596607]

Errico A, Ballabio A, Rugarli E,I. Spastin, the protein mutated in autosomal dominant hereditary spastic paraplegia, is involved in microtubule dynamics. Hum. Mol. Genet 2002;11:153–163. [PubMed: 11809724]

Evans K, Keller C, Pavur K, Glasgow K, Conn B, Lauring B. Interaction of two hereditary spastic paraplegia gene products, spastin and atlastin, suggests a common pathway for axonal maintenance. P.N.A.S 2006;103:10666–10671. [PubMed: 16815977]

Fink JK, Hedera P. Hereditary spastic paraplegia: heterogeneity and genotype/phenotype correlation. Semin. Neurol 1999;19:301–310. [PubMed: 12194386]

Fink JK. Hereditary spastic paraplegia. Curr. Neurol. Neurosci. Rep 2006;6:65–176. [PubMed: 16469273]

Goytain A, Hines R,M, El-Husseini A, Quamme G,A. *NIPA1* (SPG6), the basis for autosomal dominant form of hereditary spastic paraplegia, encodes a functional Mg^{2+} transporter. J. Biol. Chem 2007;282:8060–8068. [PubMed: 17166836]

Hazan J, Fonknechten N, Mavel D, Paternotte C, Samson D, Artiguenave F, Davoine C,S, Cruaud C, Dürr A, Wincker P, et al. Spastin, a new AAA protein, is altered in the most frequent form of autosomal dominant spastic paraplegia. Nat. Genet 1999;23:296–303. [PubMed: 10610178]

Hedera P, Fenichel G,M, Blair M, Haines J,L. Novel mutation in the SPG3A gene in an African American family with an early onset of hereditary spastic paraplegia. Arch. Neurol 2004;61:1600–1603. [PubMed: 15477516]

Hedera P, Eldevik PO, Maly P, Rainier S, Fink JK. Magnetic resonance imaging analysis of the spinal cord atrophy in autosomal dominant hereditary spastic paraplegia. Neuroradiology 2005;47:730–734. [PubMed: 16143870]

Hu J, Shibata Y, Zhu P,P, Voss C, Rismanchi N, Prinz W,A, Rapoport T,A, Blackstone C. A class of dynamin-like GTAases involved in the generation of the tubular ER network. Cell 2009;138:549–561. [PubMed: 19665976]

Kaneko S, Kawarai T, Yip E, Salehi-Rad S, Sato C, Orlacchio A, Bernardi G, Liang Y, Hasegawa H, Rogaeva E, et al. Novel SPG6 mutation p.A100T in a Japanese family with autosomal dominant form of hereditary spastic paraplegia. Mov. Disord 2006;21:1531–1533. [PubMed: 16795073]

Lee M, Paik S,K, Lee M,J, Kim Y,J, Kim S, Nahm M, Oh S,J, Kim H,M, Yim J, Lee C,J, et al. Drosophila Atlastin regulates the stability of muscle microtubules and is required for synapse development. Dev. Biol 2009;330:250–262. [PubMed: 19341724]

Lo W,Y, Botzolakis E,J, Tang X, Macdonald R,L. A conserved Cys-loop receptor aspartate residue in the M3–M4 cytoplasmic loop is required for GABAA receptor assembly. J. Biol. Chem 2008;283:29740–29752. [PubMed: 18723504]

Namekawa M, Muriel M,P, Janer A, Latouche M, Dauphin A, Debeir T, Martin E, Duyckaerts C, Prigent A, Depienne C, et al. Mutations in the SPG3A gene encoding the GTPase atlastin interfere

with vesicle trafficking in the ER/Golgi interface and Golgi morphogenesis. Mol. Cell. Neurosci 2007;35:1–13. [PubMed: 17321752]

Orso G, Pendin D, Liu S, Tosetto J, Moss T,J, Faust J,E, Micaroni M, Egorova A, Martinuzzi A, McNew J,A, et al. Homotypic fusion of ER membranes requires the dynamin-like GTPase atlastin. Nature 2009;460:978–83. [PubMed: 19633650]

Park S,H, Zhu P,P, Parker R,L, Blackstone C. Hereditary spastic paraplegia proteins REEP1, spastin, and atlastin-1 coordinate microtubule interactions with the tubular ER network. J. Clin. Invest 2010;120:1097–1110. [PubMed: 20200447]

Patel H, Cross H, Proukakis C, Hershberger R, Bork P, Ciccarelli F,D, Patton M,A, McKusick V,A, Crosby A,H. SPG20 is mutated in Troyer syndrome, an hereditary spastic paraplegia. Nature Genet 2002;4:347–348. [PubMed: 12134148]

Praefcke G,J, McMahon H,T. The dynamin superfamily: universal membrane tubulation and fission molecules? Nat. Rev. Mol. Cell. Biol 2004;5:133–147. [PubMed: 15040446]

Rainier S, Chai J,H, Tokarz D, Nicholls R,D, Fink J,K. NIPA1 gene mutations cause autosomal dominant hereditary spastic paraplegia (SPG6). Am. J. Hum. Genet 2003;73:967–971. [PubMed: 14508710]

Reed J,A, Wilkinson P,A, Patel H, Simpson M,A, Chatonnet A, Robay D, Patton M,A, Crosby A,H, Warner T,T. A novel NIPA1 mutation associated with a pure form of autosomal dominant hereditary spastic paraplegia. Neurogenetics 2005;6:79–84. [PubMed: 15711826]

Reid E. Science in motion: common molecular pathological themes emerge in the hereditary spastic paraplegias. J. Med. Genet 2003;40:81–86. [PubMed: 12566514]

Rismanchi N, Soderblom C, Stadler J, Zhu P,P, Blackstone C. Atlastin GTPase are required for Golgi apparatus and ER morphogenesis. Hum. Mol. Genet 2008;17:1591–1604. [PubMed: 18270207]

Salinas S, Proukakis C, Crosby A, Warner TT. Hereditary spastic paraplegia: clinical features and pathogenetic mechanisms. Lancet Neurol 2008;7:1127–1138. [PubMed: 19007737]

Sanderson C,M, Connell J,W, Edwards T,L, Bright N,A, Duley S, Thompson A, Luzio J,P, Reid E. Spastin and atlastin, two proteins mutated in autosomal-dominant hereditary spastic paraplegia, are binding partners. Hum. Mol. Genet 2006;5:307–318. [PubMed: 16339213]

Sauter S,M, Engel W, Neumann L,M, Kunze J, Neesen J. Novel mutations in the Atlastin gene (SPG3A) in families with autosomal dominant hereditary spastic paraplegia and evidence for late onset forms of HSP linked to the SPG3A locus. Hum. Mutat 2004;23:98. [PubMed: 14695538]

Simpson M,A, Cross H, Proukakis C, Pryde A, Hershberger R, Chatonnet A, Patton M,A, Crosby A,H. Maspardin is mutated in mast syndrome, a complicated form of hereditary spastic paraplegia associated with dementia. Am. J. Human. Genet 2003;73:1147–1156. [PubMed: 14564668]

Soderblom C, Blackstone C. Traffic accidents: molecular genetic insights into the pathogenesis of the hereditary spastic paraplegias. Pharmacol. Ther 2006;109:42–56. [PubMed: 16005518]

Tessa A, Casali C, Damiano M, Bruno C, Fortini D, Patrono C, Cricchi F, Valoppi M, Nappi G, Amabile G,A, et al. SPG3A: An additional family carrying a new atlastin mutation. Neurology 2002;59:2002–2005. [PubMed: 12499504]

Tsang H,T, Edwards T,L, Wang X, Connell J,W, Davies R,J, Durrington H,J, O'Kane C,J, Luzio J,P, Reid E. The hereditary spastic paraplegia proteins NIPA1, spastin and spartin are inhibitors of mammalian BMP signaling. Hum. Mol., Genet 2009;18:3805–3821. [PubMed: 19620182]

Wang X, Shaw W,R, Tsang H,T, Reid E, O'Kane C,J. Drosophila spichthyin inhibits BMP signaling and regulates synaptic growth and axonal microtubules. Nature Neurosci 2007;10:177–185. [PubMed: 17220882]

Wharton S,B, McDermott C,J, Grierson A,J, Wood J,D, Gelsthorpe C, Ince P,G, Shaw P,J. The cellular and molecular pathology of the motor system in hereditary spastic paraparesis due to mutation of the spastin gene. J. Neuropathol. Exp. Neurol 2003;62:1166–1177. [PubMed: 14656074]

Zhao X,P, Alvarado D, Rainier S, Lemons R, Hedera P, Weber C,H, Tukel T, Apak M, Heiman-Patterson T, Ming L, et al. Mutation in a novel GTPase cause autosomal dominant hereditary spastic paraplegia. Nat. Genet 2001;29:326–331. [PubMed: 11685207]

Zhao J, Matthies D,S, Botzolakis E,J, Macdonald R,L, Blakely R,D, Hedera P. Hereditary spastic paraplegia-associated mutations in the NIPA1 gene and its C. elegans homolog trigger neural

degeneration in vitro and in vivo through a gain of function mechanism. J. Neurosci 2008;28:13938–13951. [PubMed: 19091982]

Zhu P,P, Patterson A, Lavoie B, Stadler J, Shoeb M, Patel R, Blackstone C. Cellular localization, oligomerization, and membrane association of the hereditary spastic paraplegia 3A (SPG3A) protein atlastin. J. Biol. Chem 2003;278:49063–49071. [PubMed: 14506257]

Zhu P,P, Soderblom C, Tao-Cheng J,H, Stadler J, Blackstone C. SPG3A protein atlastin-1 is enriched in growth cones and promotes axon elongation during neuronal development. Hum. Mol. Genet 2006;15:1343–1353. [PubMed: 16537571]

Züchner S. The genetics of hereditary spastic paraplegia and implications for drug therapy. Expert Opin Pharmacother 2007;8:1433–1439. [PubMed: 17661726]

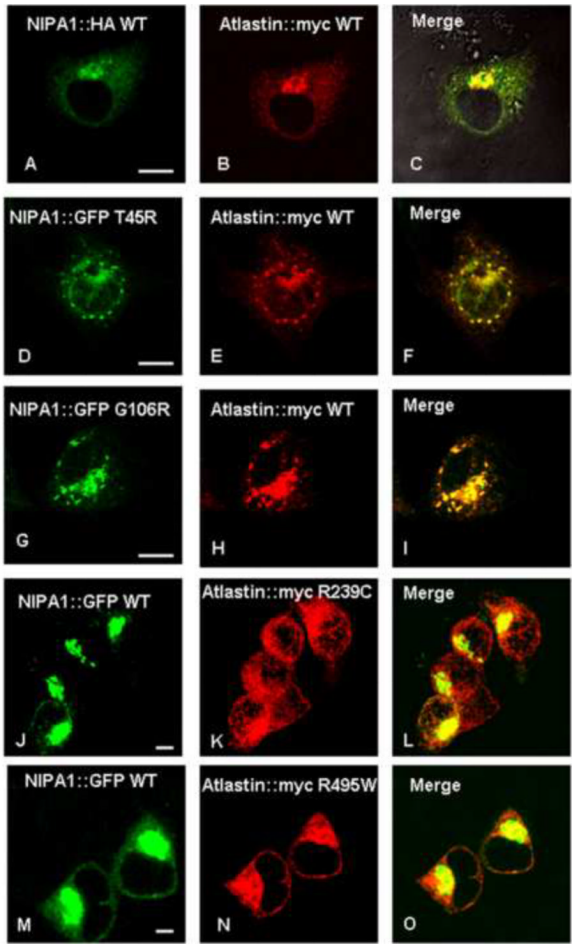

Figure 1. NIPA1 and atlastin-1 were partially colocalized and HSP mutations altered the distribution of its binding partner

Co-expressed WT NIPA1-GFP and WT atlastin-1-HA [red] demonstrated marked colocalization, consistent with the endoplasmic reticulum (ER) and trans-Golgi complex (for the confirmation of GC localization, see Figure 2) (panels A–C). Introduction of T45R and G106R HSP NIPA1 mutations resulted in alteration of the distribution patterns of WT atlastin-1 with a nodular accumulation of both mutant forms of NIPA1 and WT atlastin-1 (panels D–I); these aggregates were localized in ER (see also Figure 2). Coexpression of mutant forms of atlastin-1 and WT NIPA1 also resulted in altered subcellular distribution of both mutant NIPA1 and WT atlastin-1. Both R239C and R495W mutations resulted in the formation of thick bundles of mutant atlastin-1 in the cytoplasm, and both atlastin-1 mutations in the increased NIPA1 signal from the CG complex (panels J–O) (see also Figure 2). Scale bar = 5μm.

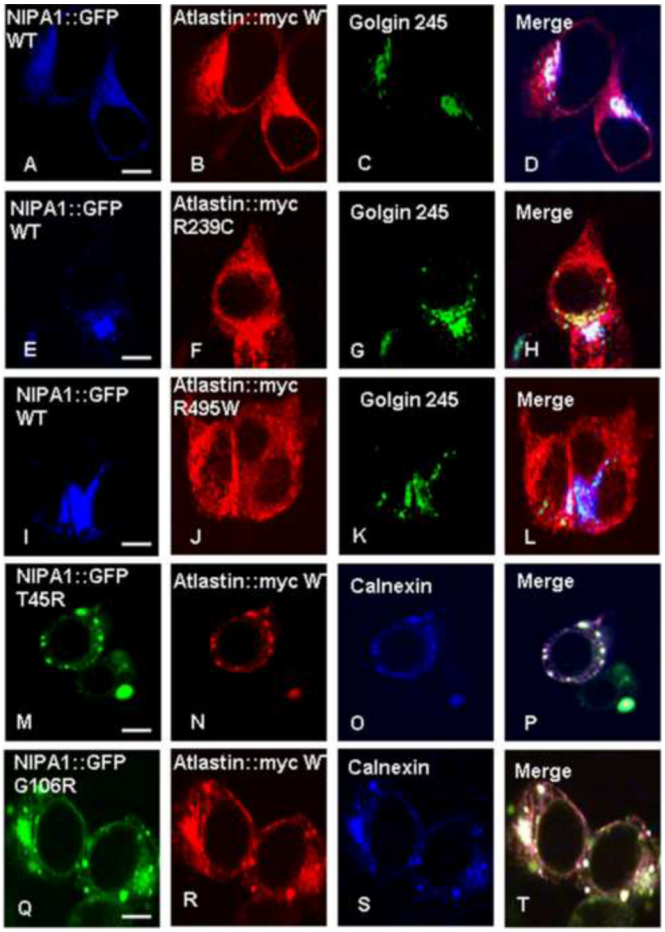

Figure 2. The presence of mutant forms of binding partners caused sequestration of WT NIPA1 in GC and WT atlastin-1 in ER

Triple immunostaining confirming the colocalization in GC complex of both WT forms of proteins (panels A–D) and in ER (panels A–D, calnexin co-staining not shown). We also observed an accumulation of WT NIPA1 in GC in the presence of studied HSP atlastin-1 mutations (panels E–L), and accumulation of WT atlastin-1 in ER together with mutant forms of NIPA1 (panels M–U). Scale bar = 5μm.

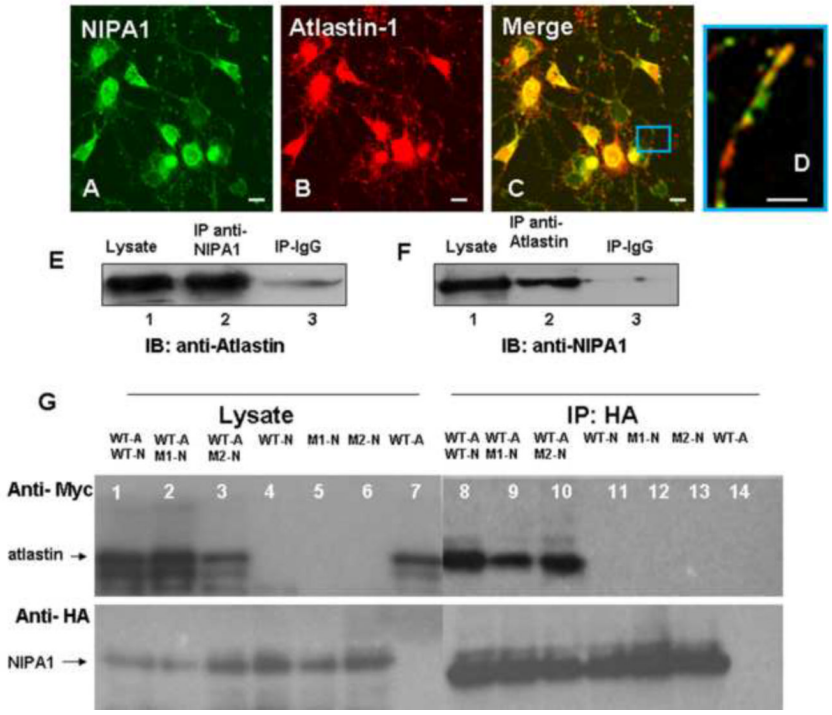

Figure 3. Atlastin-1 and NIPA1 are binding partners

Staining with anti-NIPA1 antibodies (panel A, green) and anti-atlastin-1 (red, panel B) demonstrated a significant colocalization of endogenous NIPA1 and atlastin-1 proteins in cultured E18 cortical rat neurons (panel C, overlay, panel D – detail of axon). The whole mouse brain extracts proteins were immunoprecipitated (IP) with NIPA1 antibodies or control IgG and analyzed by immunoblotting (IB) with atlastin-1 antibodies (panel E). Similarly, IP with atlastin-1 antibodies and IB with anti-NIPA1 antibodies showed similar results (panel F).

Co-immunoprecipitation of tagged WT atlastin-1-myc (panel G, lanes 1, 2, 3 and 7; upper panel) and NIPA1-HA (lower panel) using anti-HA antibodies from transfected COS-7 cells; lanes 1, 8 and 11 contain WT NIPA1, lanes 2, 9 and 12 T45R NIPA1 mutation, and lanes 3, 6, and 13 G106R NIP1 mutation. Co-immunoprecipitation was observed in lanes 8–10 and NIPA1 mutations did not affect the affinity of both proteins. Similarly, R239C and R495W atlastin-1 mutations did not alter co-immunoprecipitation with WT NIPA1 (data not shown). Lanes 7 and 14 represent a negative control in the absence of NIPA1. (Legend: WT-A = wild type atlastin-1, WT-N = wild type NIPA1, M1-N = T45R NIPA1, M2-N = G106R NIPA1). Scale bar = 5μm.

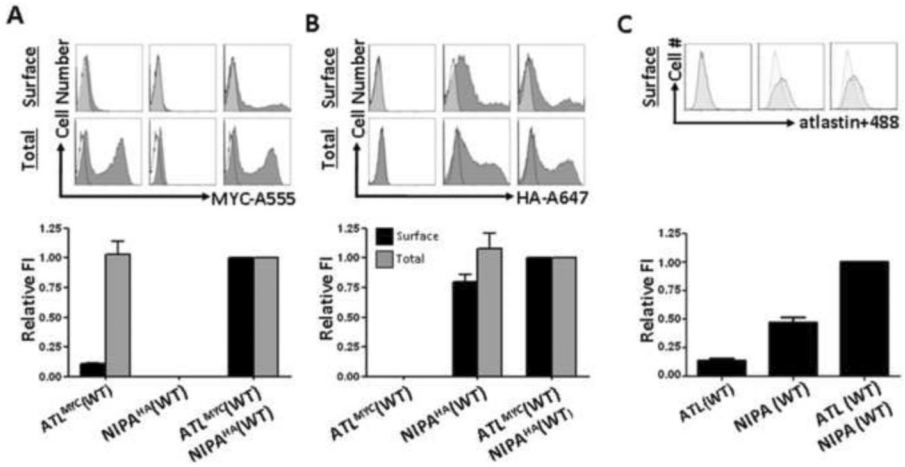

Figure 4. The presence of NIPA1 facilitated trafficking of atlastin-1 to the cell surface

Representative flow cytometry frequency histograms of Alexa-555 (A555) fluorescence intensity for cells expressing atlastin-1-myc (A, upper row), Alexa-647 (A647) fluorescence intensity for cells expressing NIPA1-HA (B, upper row), and atlastin-1 antibodies with Alexa-488 secondary antibodies (panel C, upper row). A representative histogram from mock transfected cells (white) was overlaid on each of the histograms from positively transfected cells (grey). The x-axis indicates arbitrary fluorescence units (log scale) and the y-axis indicates the number of cells.

Lower row shows plotting of the surface and total expression of tagged atlastin-1 (panel A), NIPA1 (panel B) and atlastin-1 antibodies (panel C) on the cell surface. Surface staining (without membrane permeabilization) is depicted by black columns and total cellular staining (after membrane permeabilization) is depicted as gray columns. Co-transfection of atlastin-1-myc and NIPA1-HA resulted in approximately 10-fold increase of cell surface activity without changing the total amount of expressed atlastin-1. Same pattern was observed when we used direct atlastin-1 antibodies (panel C).

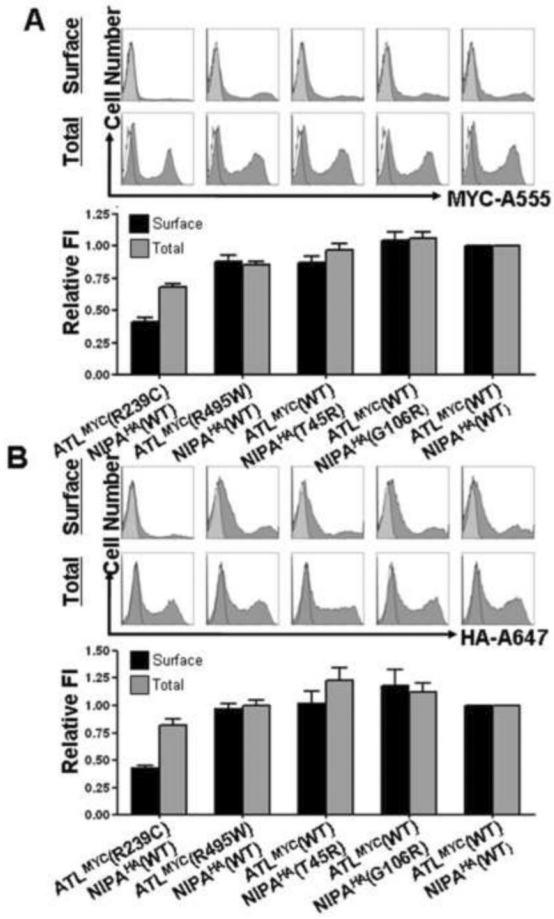

Figure 5. Atlastin-1 mutations exhibited a dominant-negative effect on NIPA1 cell surface trafficking

Representative flow cytometry frequency histograms of Alexa-555 (A555) fluorescence intensity and plotting of cell surface and total signal of atlastin-1-myc (panel A), and representative flow cytometry frequency histograms of Alexa-647 (A647) fluorescence intensity for cells expressing NIPA1-HA (panel B). A representative histogram from mock transfected cells (white) was overlaid on each of the histograms from positively transfected cells (grey). Surface staining (without membrane permeabilization) is shown as gray columns and total cellular staining (after membrane permeabilization) is shown as black columns. The x-axis indicates arbitrary fluorescence units (log scale) and the y-axis indicates the number of cells.

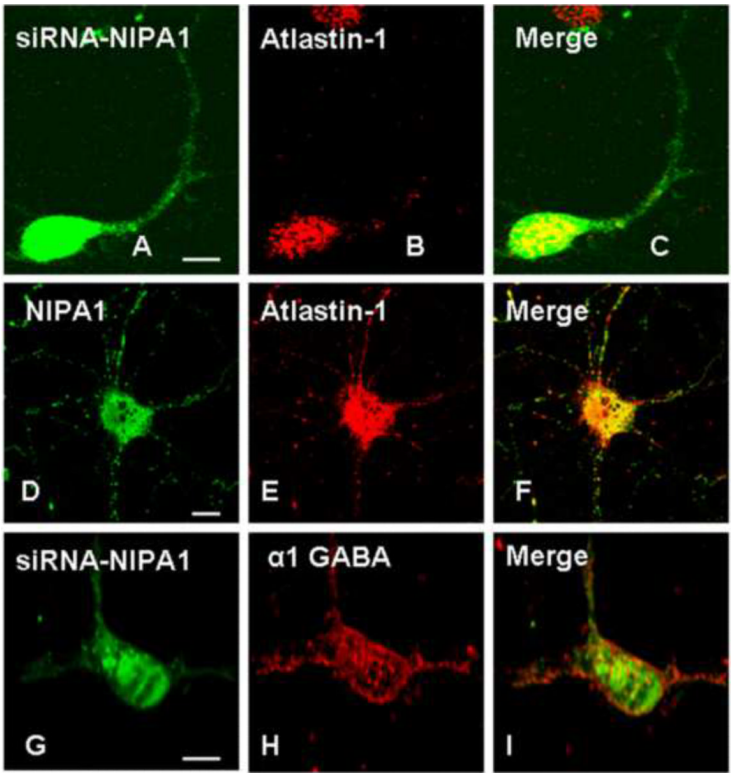

Figure 6. Depletion of endogenous NIPA1 in rat neurons altered the distribution of endogenous atlastin-1 protein

Expression of siRNA2 (panels A–C) in cultured cortical rat neurons targeting NIPA1, indicated by expression of GFP in neuronal cells (panel A) resulted in markedly altered intracellular distribution of endogenous atlastin-1 (panel B, red) with clumping of the atlastin-1 protein in the neuronal body, and its noticeable absence on the cell surface and in the neuronal processes (panel C, overlay). Normal distribution of endogenous atlastin-1 in the same types of cells is again shown in panels D–F (D shows endogenous NIPA1, E endogenous atlastin-1, and F overlay). Expression of siRNA did not non-specifically disrupt secretory pathway because cell surface trafficking of the the $GABA_A$ receptor α1 subunit was not altered when compared to control neurons (panel G expression of siRNA2 targeting NIPA1, panel H endogenous α-1 $GABR_A$ [red], panel I overlay; negative controls not shown). Scale bar = 10μm.

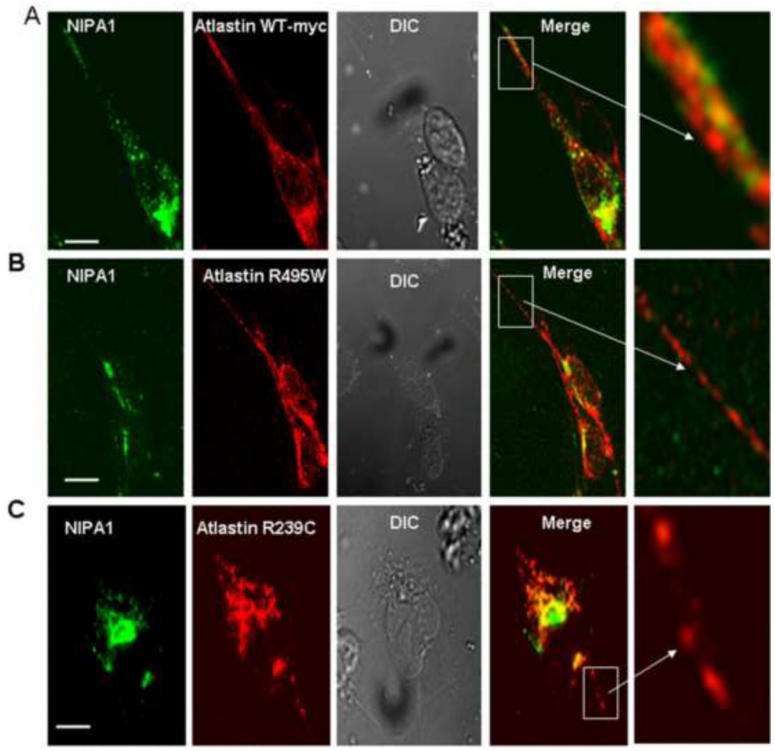

Figure 7. Expression of mutant forms of atlastin-1 altered distribution of endogenous NIPA1

Endogenous WT NIPA1 in cultured cortical rat neurons showed a similar pattern, as was seen in heterologous cell lines, of colocalization with myc-tagged WT atlastin-1 protein in the neuronal bodies (Panel A, green anti-NIPA1 antibodies, red anti-myc antibodies). Endogenous WT NIPA1 was also transported to axons, where is partially colocalized with WT atlastin-1 (panel A, 5th row). Expression of studied HSP mutations dramatically redistributed endogenous WT NIPA1 (see also Figure 8) with a nearly complete disappearance of NIPA1 signal from neuronal axons and apparently thinner axons (Panel B R495W atlastin-1-myc, panel C, R239C atlastin-1-myc, antibodies same as for panel A). Scale bar = 10μm.

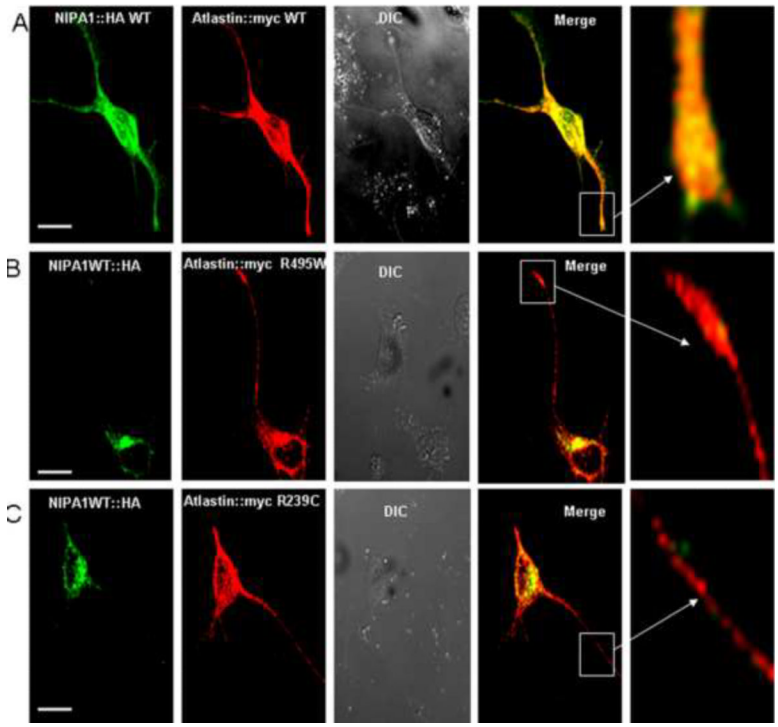

Figure 8. Overexpression of WT NIPA1 did not compensate for the effect of mutant forms of atlastin-1

Overexpression of WT NIPA1 did not alter the patters illustrated in Figure 7 and the sequestration of WT NIPA1 in the neuronal bodies was again seen after the introduction of HSP atlastin-1 mutations. Panel A shows distribution of co-expressed WT NIPA1-HA and WT atlastin-1-myc proteins (green anti-HA antibodies, red anti-myc antibodies). Panels B (expressed mutation R495W atlastin-1-myc) and C (expressed mutation R239C atlastin-1-myc) demonstrate markedly altered intracellular distribution of expressed WT NIPA1 with its absence from axons. Scale bar = 10μm.

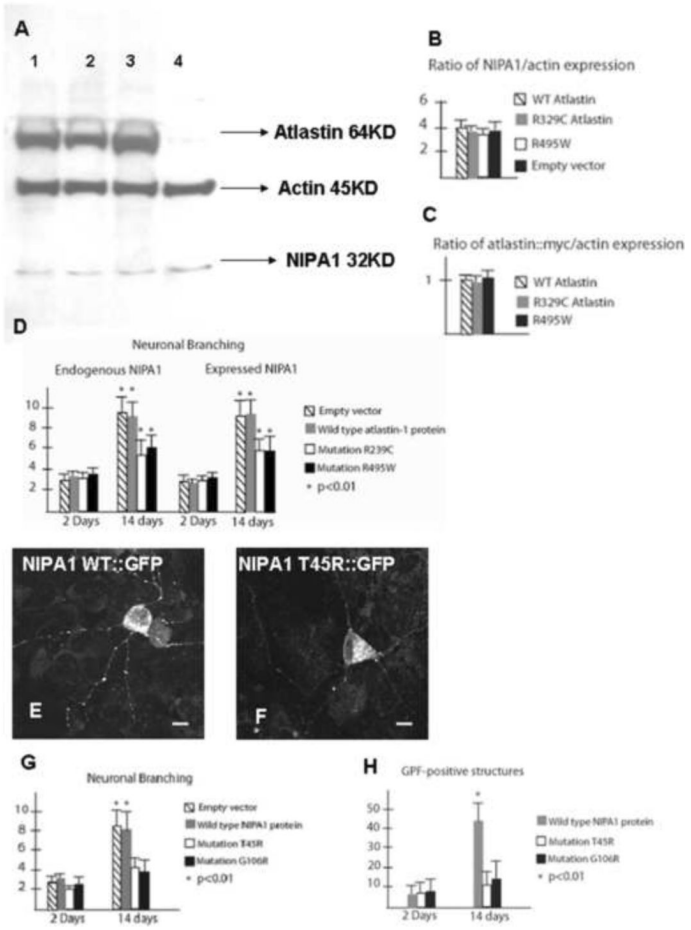

Figure 9. Neuronal branching was reduced in the presence of mutant forms of NIPA1 and atlastin-1

Western blot analysis of endogenous NIPA1 expression did not show any reduction of total expression in the presence of mutant forms of atlastin-1 (panel A; atlastin-1-myc detected with anti-myc antibodies, NIPA1 with anti-NIPA1 antibodies, lane 1 WT atlastin-1, lane 2 R329C atlastin-1-myc, lane 3 R495W atlastin-1-myc, lane 4 empty vector). Both mutant forms of atlastin-1 had a robust expression, which did not differ from WT form (panels B and C ratio of NIPA1 and actin intensity).

Panel D shows plotting of neuronal branching of cultured cortical rat neurons expressing R239C and R495W atlastin-1 mutations, and with normal (endogenous) levels of WT NIPA1 (first two plots from left) and overexpressed WT NIPA1 (3rd and 4th plots from left). Neuronal branching assessed two weeks after transfection showed statistically significant reduction of neuronal branching of axons and dendrites, which was very similar for both mutations and was not modified by overexpressed WT NIPA1 (y-axis shows the sum of counted primary and secondary branching, striped bar empty vector, gray bar WT atlastin-1-myc, white bar R239C atlastin-1-myc, black bar R495W atlastin-1-myc).

Rat cortical neurons expressing WT NIPA1-GFP showed abundant presence of GFP-positive structures in neuronal processes assessed 14 days after transfection (panel E). Neurons expressing mutant forms of NIPA1 protein showed reduced number of GFP-positive structures assessed two weeks after transfection (panel F).

Panel G shows plotting of neuronal branching of cultured rat neurons expressing WT NIPA1-GFP, T45R NIPA1-GFP and G106R NIPA1-GFP two days after transfection and two weeks after transfection (y-axis as above, striped bar empty vector, gray bar WT

NIPA1-GFP, white bar T45R NIPA1-GFP, black bar G106R NIPA1-GFP, * $p<0.01$). Panel H shows plotting of GFP-positive structures ($p<0.001$) in neuronal processes (y-axis shows estimated numbers of GFP-positive structures, bar coloring same as for panel G). Scale bar = 5 μm.